Front.Comput.Sci.
DOI

RESEARCH ARTICLE

Numerical Evaluation on Sub-Nyquist Spectrum Reconstruction Methods

Zihang SONG [1], Han ZHANG [1], Sean FULLER [2], Andrew LAMBERT [3], Zhinong YING [4], Petri MAHONEN [5,6], Yonina ELDAR [7], Shuguang CUI [8], Mark D. PLUMBLEY [1], Clive PARINI [9], Arumugam NALLANATHAN [9], Yue GAO (✉)[1]

1 School of Computer Science and Electronic Engineering, University of Surrey, Guildford, Surrey GU2 7XH, United Kingdom
2 National Instruments Corporation (UK) Ltd, Newbury, Berkshire RG14 2PZ, United Kingdom
3 Electronic Media Services Ltd, Bordon, Hampshire GU35 0FJ, United Kingdom
4 Sony Research Center, Sony Corporation, 221 88 Lund, Sweden
5 Institute for Networked Systems, RWTH Aachen University, Kackertstrasse 9, 52072 Aachen, Germany
6 Aalto University, School of Electrical Engineering, Department of Communications and Networking, 02150 Espoo, Finland
7 Faculty of Math & CS, Weizmann institute of Science, Rehovot 7610001, Israel
8 School of Science and Engineering, The Chinese University of Hong Kong (Shenzhen), 518172, China
9 School of Electronic Engineering and Computer Science, Queen Mary University of London, London E1 4NS, United Kingdom

Abstract The compressed spectrum sensing technique substantially reduces the hardware requirements for wideband sensing by utilizing reconstruction algorithms to reconstruct the spectrum from the sub-Nyquist sampling sequence. This paper introduces a basic framework of sub-Nyquist sampling, outlines the reconstruction techniques of compressed sensing theory, and contrasts the pros and cons of optimization, greedy, sparse Bayesian learning, and non-sparse approximation algorithms. In light of the results of the GBSense Challenge 2021, four spectrum reconstruction algorithms are chosen for numerical evaluation, and their reconstruction accuracy and computational efficiency are examined. The results of this paper have reference significance for the practice of wideband compressed spectrum sensing.

Keywords compressed sensing, wideband spectrum sensing, reconstruction algorithm

Received month dd, yyyy; accepted month dd, yyyy

E-mail: yue.gao@surrey.ac.uk

1 Introduction

1.1 Background

The increasing number of users and the demand for improved quality of service (QoS) have been the driving forces behind the rapid growth of the wireless industry. In the meantime, the increase in the number of users and their throughput places more demands on wireless spectrum resources. A substantial amount of the available spectrum is reserved for licensed primary users (PUs). However, the rate of licensed spectrum occupancy in time and space remains low. Spectrum monitoring data collected on a global basis indicates that the licensed spectrum is utilized by the PU for just 5 to 10 percent of the time [1].

When the licensed frequency range is not fully utilized by PUs, a significant number of spectrum holes appear. The emergence of cognitive radio (CR) technology enables unlicensed secondary users (SUs) to temporarily occupy the frequency holes for communication, hence facilitating the intelligent, optimum, and equitable utilization and sharing of spectrum resources [2].

Spectrum sensing, as a crucial technique for CR devices, enables SUs constantly monitor all nearby spectrum bands to detect the emergence of PU signals and spectrum holes. As the working bandwidth of CR equipment continues to expand, spectrum sensing encounters tough hardware limitations, necessitating the use of very high-speed analog to digital converters (ADCs), which can be more expensive and energy-intensive.

Benefiting from the sparse character of the wideband spectrum, compressed sensing (CS) theory has been applied to the wideband spectrum sensing task, spawning the interdisciplinary area of compressed spectrum sensing (CSS). CSS is anticipated to overcome the hardware limits of spectrum sensing by employing sub-Nyquist rate sampling units and CS reconstruction algorithms, whilst avoiding high power consumption and high cost.

Researches on CSS can be primarily subdivided into 1) sub-Nyquist sampling methods, 2) signal recovery algorithms, and 3) channel detection techniques. Some well-known sampling architectures, such as the random demodulator [3,4], the modulated wideband converter (MWC) [5–7], and the multicoset sampler [8,9], have been extensively studied and proven to be efficient and hardware-friendly. On the other hand, the performance of channel detection methods is highly dependent on the spectrum reconstruction results [10–13]. Consequently, spectrum reconstruction methods play a significant role in the successful access of SUs to spectrum holes.

Three types of reconstruction algorithms, namely greedy matching pursuit, optimization, and Bayesian-based methods [14–17], have already been introduced and widely used in CSS. However, shortcomings usually come along with the advantages for every type of algorithm. Greedy algorithms are computationally efficient, but provide no guarantee for successful support recovery and require prior knowledge on the signal [18–20]. Optimization methods, especially convex relaxations, usually provide theoretical guarantees for exact recovery given the sensing matrix satisfying certain restricted isometry property (RIP), but are featured by high computational complexity [21]. The Bayesian-based techniques approach the sparse reconstruction problem as a maximum likelihood approximation problem based on assumptions about signal and noise distributions. When the assumptions are met, accurate findings are achievable, and vice versa.

Nonetheless, there is a significant opportunity for further development of reconstruction algorithms. First, there is still a significant gap between the sample resources required by existing algorithms and the theoretical lower bound [22], indicating that not all of the information contained in the subsampling sequence has been mined. In addition, when the signal-to-noise ratio deteriorates, the performance of the majority of reconstruction algorithms decreases substantially. Moreover, the complexity of existing algorithms is still considerable. Even greedy algorithms fall short of the requisite efficiency for real-time spectrum sensing [23,24].

1.2 GBSense project and the affiliated challenge

The EPSRC fellowship project “GHz Bandwidth Sensing” (GBSense) proposes a novel method for designing GHz bandwidth sensing systems to overcome the Nyquist-rate sampling bottleneck by developing sub-Nyquist sampling algorithms and reusing the existing knowledge of smart antennas and reconfigurable transmission lines [25]. Without necessitating Nyquist-rate sampling, the GBSense provides new innovative and implementable options on a real-time experimental platform. The GBSense provides users with a hardware platform and application software that enables real-time over-the-air GHz bandwidth signal sensing, processing, and transmission at both sub-6GHz and mm-wave frequency bands. It will also interface with a low-cost computing unit, such as Raspberry PI, where sub-Nyquist algorithms are hosted in order to improve human-computer interaction, increase the current understanding of sub-Nyquist sampling theory, and present new challenges to software and hardware engineers.

The GBSense Challenge 2021, affiliated with the GBSense project, was held in March 2021 [25], focusing on the development of sub-Nyquist reconstruction algorithms. The GBsense Challenge 2021 was issued with open datasets and a reference sub-Nyquist data-processing framework. Several entries were selected and evaluated by a panel composed of leading experts in the field. Four algorithms were shortlisted for the GBSense awards, namely the “Slow Kill” (SK) method [26–28], subspace-augmented simultaneous orthogonal matching pursuit (SA-SOMP) [29], multiple sparse Bayesian learning (MSBL) [30] and fast compressed power spectrum estimation (FCPSE) [31]. The selected four algorithms are innovative and representative in their respective categories.

1.3 Outline

The rest of the paper is composed as follows. In section 2, the fundamental multiband signal model and sampling architecture are introduced. In section 3, the algorithms presented by the GBSense Challenge 2021 finalists are classified and described, along with two benchmarks representing typical greedy algorithms, namely simultaneous orthogonal matching pursuit (SOMP) and joint-block hard threshold pursuit (JB-HTP). The platform utilized for generating the test datasets and evaluating the algorithms is introduced in section 4. Using the shortlisted algorithms, numerical experiments are undertaken in section 5. The paper concludes with the experimental assessment outcome and its conclusion.

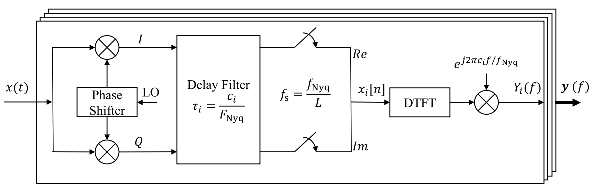

Fig. 1 The diagram of the basic implementation of multicoset sampler.

2 Signal and System Models

2.1 Signal Model

We adopt the widely-known multiband signal model which describes N_{sig} complex transmissions located in the baseband of interest $\mathcal{F} = [-f_{\mathrm{Nyq}}/2, f_{\mathrm{Nyq}}/2]$, where f_{Nyq} correspond to the baseband Nyquist frequency. Each transmission is assumed to be of bandwidth no larger than B and not overlapping with other transmissions without loss of generality.

Consider a wideband cognitive receiver that is passively sensing the spectrum upon $\mathcal{F}$. At the receiver baseband, the received signal is modeled in temporal domain as

$$x(t) = \sum_{i \in N_{\mathrm{sig}}} s_i(t) + n(t) \tag{1}$$

where $s_i(t)$ denotes the i^{th} transmission signal containing all the channel effects, and $n(t)$ denotes additive Gaussian noise. In this work, the baseband signal is assumed to be sparse in the frequency domain, i.e., $N_{\mathrm{sig}} B \ll f_{\mathrm{Nyq}}$.

2.2 Multicoset Sampling

The cognitive receiver is assumed to be equipped with a well-known periodic non-uniform sampling architecture, known as the multicoset sampler [8], to acquire the baseband signal samples at a sub-Nyquist rate. The basic structure of a multicoset sampler is shown in Fig. 1. A power splitter divide the analog signal into p ways (referred as "cosets" afterwards) and impose different analog delays $\tau_i = c_i/f_{\mathrm{Nyq}}$ specified by the delay pattern $C = \{c_i \in \mathbb{Z} \mid 0 \leq c_i < L, i = 1, 2, ..., p\}$ to each coset of the signal. Then each coset of the signal is digitized by a low-rate ADC working at a sampling rate $f_s = f_{\mathrm{Nyq}}/L$, where integer L satisfies $L > p$ to ensure compressed sampling. The sample sequence acquired in the i^{th} coset is expressed as

$$x_i[n] = x\left(\frac{nL}{f_{\mathrm{Nyq}}} + \frac{c_i}{f_{\mathrm{Nyq}}}\right), \quad n \in \mathbb{Z}. \tag{2}$$

It makes sense that the samples we obtain from each coset are a downsampled version of the Nyquist samples with a downsampling coefficient L, and the overall average sampling rate of the multicoset sampler is $p f_{\mathrm{Nyq}}/L$. By denoting the i^{th} measurement as

$$Y_i(f) = \frac{L}{f_{\mathrm{Nyq}}} e^{-j2\pi c_i T_{\mathrm{Nyq}} f} X_i(e^{j2\pi f L/f_{\mathrm{Nyq}}}) \tag{3}$$

where $X_i\left(e^{j2\pi f L/f_{\mathrm{Nyq}}}\right) = \sum_{n=-\infty}^{\infty} x_i[n] e^{-j2\pi f L n/f_{\mathrm{Nyq}}}$ is the discrete-time Fourier transform (DTFT), we can establish a linkage between the compressed measurement and the original spectrum $X(f)$, given as

$$Y_i(f) = \sum_{n=-\lfloor \frac{L}{2} \rfloor}^{+\lfloor \frac{L}{2} \rfloor - 1} X\left(f + \frac{n f_{\mathrm{Nyq}}}{L}\right) \exp\left(j2\pi \frac{n c_i}{L}\right). \tag{4}$$

Equation (4) indicates that the measurement $Y_i(f)$ in the i^{th} coset can be represented by a linear combination of L separate samples on the signal's original spectrum $X(f)$. By stacking the p single-coset measurements columnwise we get the matrix form the linkage

$$\mathbf{y}(f) = \mathbf{A}\mathbf{x}(f) \tag{5}$$

where $\mathbf{y}(f) = [Y_1(f) \quad Y_2(f) \quad ... \quad Y_p(f)]^{\mathrm{T}}$ and $\mathbf{x}(f)$ is a column vector of length L composed of $\{X(f + n f_{\mathrm{Nyq}}/L) | n = 0, 1, ..., L-1\}$. The coefficient matrix $\mathbf{A}$ is a $p \times L$ matrix whose il^{th} element is given by

$$A_{i,l} = e^{j2\pi c_i (-2/L + l - 1)/L}. \tag{6}$$

In practice, a finite window is usually employed and discrete Fourier transform (DFT) is actually used instead of DTFT. Denoting the window length as N per coset, a multiple measurement vectors (MMV) model

$$\mathbf{Y} = \mathbf{A}\mathbf{X} \tag{7}$$

can be derived, where $\mathbf{Y}$ is a $p \times N$ measurement matrix whose $(i, n)^{\mathrm{th}}$ element is

$$Y_{i,n} = Y_i\left((n-1) f_{\mathrm{Nyq}}/NL\right), \tag{8}$$

and $\mathbf{X}$ is a $L \times N$ matrix whose $(l, n)^{\mathrm{th}}$ element is

$$X_{l,n} = X\left(\frac{-L/2 + l - 1 + (n-1)/N}{L/f_{\mathrm{Nyq}}}\right). \tag{9}$$

2.3 Problem Formulation

The problem of solving equation (7) can be regarded as a decomposition problem, where $\mathbf{A}$ is a $p \times L$ dictionary matrix , $\mathbf{Y}$ is a $p \times N$ measurement matrix composed of N individual p-dimensional measurement vectors, and the $L \times N$ matrix $\mathbf{X}$ contains the coefficients of columns (atoms) in $\mathbf{A}$ to be estimated.

In the case $P < L$, $\mathbf{A}$ is an overcomplete dictionary, and (7) is undetermined with infinite solutions of $\mathbf{X}$. With the block-sparse nature of the spectrum, $\mathbf{X}$ is usually regarded as a joint-sparse coefficient matrix where each of its column shares a same support [15]. Thus, solving (7) is transformed into a l_0-norm minimization problem

$$\min_{\mathbf{X}\in\mathbb{C}^{L\times N}} \|\mathbf{X}\|_0 \;\; \text{s.t.} \;\; \mathbf{Y} = \mathbf{A}\mathbf{X}. \tag{10}$$

In practice the measurement $\mathbf{Y}$ is unavoidably perturbed by noise. Thus a common relaxation on (10) is to give a l_2-norm-bounded error tolerance ϵ:

$$\arg\min_{\mathbf{X}\in\mathbb{C}^{L\times N}} \|\mathbf{X}\|_0 \;\; \text{s.t.} \;\; \|\mathbf{Y} - \mathbf{A}\mathbf{X}\|_2 < \epsilon. \tag{11}$$

Solving both (10) and (11) is NP-hard because the discontinuity of l_0-norm [32]. Nevertheless, several computationally tractable algorithms have been proposed to approximate sparse approximation problems, and most of them have been widely applied in practice with reliable output [9, 15]. In the next section, we briefly introduce three main types of sparse approximation methods and one type of non-sparse approximation method from sub-Nyquist samples, with a detailed inspection of the symbolic algorithms submitted by the GB-Sense Challenge participants.

3 Algorithms

3.1 Greedy Algorithms

The greedy iterative algorithm is proposed for solving combinatorial optimization problems. This type of algorithm mainly uses the connection between the signal and the atomic dictionary as a way to measure whether the atom is more effective or its coefficient is non-zero. The basic principle is to iteratively find the support set of the sparse vector, and use the constrained support least squares estimation to reconstruct the signal. Such algorithms include matching pursuit (MP), orthogonal matching pursuit (OMP), stagewise orthogonal matching pursuit (StOMP), compressive sampling matching pursuit (CoSaMP), iterative hard thresholding (IHT), and gradient descent with sparsification (GraDeS), etc [15, 18–20]. The complexity of the algorithm is mainly determined by the number of iterations required to find the correct support set. The algorithm is fast in calculation but has relatively low precision.

Greedy algorithms can be easily transformed to solve MMV problems from the single measurement vector (SMV) form. SOMP treats each column of $\mathbf{X}$ and $\mathbf{Y}$ as sharing the same structure, thus accelerating the convergence when dealing with joint-sparse signals [19]. In each iteration, the most relevant atom in $\mathbf{A}$ to the residual is selected, then the residual is updated according to all the selected atoms to ensure orthogonality and to accelerate fast convergence. The JB-HTP algorithm [15] achieves fewer iterations than SOMP when processing large-size problems where $\hat{\kappa}$ is not that small. Compared to SOMP, which selects one atom in one iteration cycle, JB-HTP selects the $\hat{\kappa}$ most relevant atoms simultaneously in each iteration and converges when the selected entries are identified in two consecutive iterations. JB-HTP usually converges in very few iterations depending on the noise level. As a consequence of selecting multiple atoms at one time, its precision is lower than that of SOMP.

Based on the SOMP algorithm, the SA-SOMP [29] further relieves the computational burden without losing detection performance. The major update is to strip the noise components from the correlation matrix before the matching iterations, then the dimension of the problem can be largely reduced. SA-SOMP requires a good knowledge of signal sparsity $\hat{\kappa}$ or the noise variance to achieve ideal performance. The detailed procedures of SA-SOMP are shown in algorithm 1, where RREVD$(\mathbf{R}, \hat{\kappa})$ refers to rank-revealing eigenvalue decomposition of $\mathbf{R}$ by rank $\hat{\kappa}$.

Algorithm 1 SA-SOMP algorithm [29]

Input: $\mathbf{Y}$; $\mathbf{A} \in \mathbb{C}^{p\times L}$; $\hat{\kappa}$
Output: $\hat{\mathcal{S}}$, $\hat{\mathbf{\Theta}}$

```
R ← 𝔼[Y(f) Y^H(f)]
[U_s, Λ_s] ← RREVD(R, κ̂), χ_s ← U_s √Λ_s
t ← 1; R_0 ← χ_s; Ŝ_0 ← ∅; A_0 ← ∅;
while t ≤ κ̂ do
    α̂_t ← arg max_i ‖A^H_{:,i} R_{t−1}‖_2, i = 0, 1, ··· , L − 1
    Ŝ_t ← Ŝ_{t−1} ∪ α̂_t
    A_t ← A_{Ŝ_t}
    Θ̂_t ← arg min_ν ‖Y − A_t Θ̂_t‖_2
    R_t ← Y − A_t Θ̂_t
    t ← t + 1
end while
Ŝ ← Ŝ_t
fill the rows of Θ̂ indexed by Ŝ with Θ̂_t
```

3.2 Optimization Algorithms

The l_0 optimization problem (10) can be relaxed as convex optimization problems to find the approximate solution. The most commonly used method is the basic pursuit (BP) strategy [33]. The strategy proposes to use the l_1-norm instead of the l_0-norm to solve the optimization problem so that it can be performed using a linear programming method. For MMV problems, if joint sparsity or block sparsity is applied, the group l_1 norm optimization strategy is usually adopted by BP. Another approach is the FOCUSS algorithm, which uses the l_p-norm ($p <= 1$) instead of the l_0-norm [34]. This type of algorithm is computationally slow (computational complexity is N^3), but requires fewer measurement data ($O(K{*}\log(N/K))$ and has high accuracy. The other two more common convex relaxation algorithms include gradient projection for sparse reconstruction (GPSR) algorithm [35] and sparse reconstruction by separable approximation (SpaRSA) algorithm [36]. The GPSR algorithm solves a bounded constrained optimization problem by using gradient descent, and the algorithm requires projection in the feasible region to ensure the feasibility of the iterative process.

Proposed by She et al., the "slow kill" (SK) algorithm considers an "l_0-constrained, l_2-penalized" optimization problem to estimate the coefficient matrix $\mathbf{X}$:

$$\underset{\mathbf{X}\in\mathbb{C}^{L\times N}}{\arg\min} \ \ \|\mathbf{Y}-\mathbf{A}\mathbf{X}\|_F^2 + \frac{\eta_0}{2}\|\mathbf{X}\|_F^2 \ \text{ s.t. } \ \|\mathbf{X}\|_{2,0} \le \hat{\kappa}. \tag{12}$$

To tackle the computational and statistical challenges of the non-convex and discrete nature of problem 12, the SK algorithm adopt iteration-varying learning rate, adaptive l_2-shrinkage and progressive strategies base on an l_0-optimization approach [26–28]. The SK algorithm follows a "bottom-up" design to grow up a model from null and iterate updates the model based on a sound criterion.

3.3 Bayesian Framework

The third type of algorithm is the reconstruction algorithm based on the Bayesian framework. This type of algorithm takes into account the time correlation of the signal, especially when the signal has a strong time correlation, it can provide better than other reconstruction algorithms. Reconstruction accuracy. At present, such algorithms include: Expectation-Maximization (EM) algorithm, Bayesian compressive sensing (BCS) algorithm, sparse Bayesian learning (SBL) algorithm based on SMV model, and multiple measurement vectors (MMV) model proposed MSBL algorithm [30, 37–39]. SBL is a very important class of algorithms in Bayesian learning. The difference between MSBL algorithm and group l_1-norm convex optimization algorithm is that the latter global minimization is usually not the most sparse solution, while the former's global minima are the most sparse solution. The detailed procedure of MSBL is given in algorithm 2.

Algorithm 2 MSBL algorithm [37]

Input: $\mathbf{Y}$; $\mathbf{A}\in\mathbb{C}^{p\times L}$; σ^2; θ, *maxIter*
Output: $\hat{\mathcal{S}}$, $\hat{\mathbf{\Theta}}$

1: $\boldsymbol{\gamma}\leftarrow\mathbf{1}$; $\mathbf{\Gamma}\leftarrow\text{diag}(\boldsymbol{\gamma})$; σ^2
2: **while** $t\le maxIter$ **do**
3: $\quad\boldsymbol{\mu}\leftarrow\mathbf{\Gamma}A^{\mathrm{H}}(A\mathbf{\Gamma}A^{\mathrm{H}}+\sigma^2\mathbf{I})^{-1}\mathbf{Y}$
4: $\quad\mathbf{\Sigma}\leftarrow\mathbf{\Gamma}-\mathbf{\Gamma}A^{\mathrm{H}}(A\mathbf{\Gamma}A^{\mathrm{H}}+\sigma^2\mathbf{I})^{-1}A\mathbf{\Gamma}$
5: $\quad\gamma_i\leftarrow\frac{\frac{L}{N}\|\boldsymbol{\mu}(i,:)\|^2}{1-\mathbf{\Sigma}(i,i)/\gamma_i}$, for $i=1,2,\cdots,L$
6: $\quad\sigma^2\leftarrow\frac{\frac{L}{N}\|\boldsymbol{Y}-A\boldsymbol{\mu}\|_F^2}{p-L+\text{Tr}(\mathbf{\Gamma}^{-1}\mathbf{\Sigma})}$
7: $\quad\mathbf{\Gamma}\leftarrow\text{diag}(\boldsymbol{\gamma})$
8: **end while**
9: Let $\hat{\mathcal{S}}$ be the set of all index i such that $\gamma_i\ge\frac{\theta}{L}\sum_{i=1}^{L}\gamma_i$
10: $\hat{\mathbf{\Theta}}(\hat{\mathcal{S}},:)\leftarrow\boldsymbol{\mu}(\hat{\mathcal{S}},:)$, $\hat{\mathbf{\Theta}}(\hat{\mathcal{S}}^c,:)\leftarrow\mathbf{0}$

3.4 Non-sparse reconstruction

The fast compressed power spectrum estimation (FCPSE) seeks for another approach to estimating the power spectrum from an incomplete sampling sequence [31], sh shown in algorithm 3. FCPSE acquires an approximation of the covariance matrix directly from the zero-filling upsampled version of the multicoset sampling sequence. To avoid vacant elements in the covariance, the multicoset sampling delay pattern must be specifically designed, and the minimum average sampling rate should be above half the Nyquist rate. The output sequence $\hat{\boldsymbol{\theta}}$ can be regard as an unbiased estimation of the real power spectrum $\boldsymbol{\theta}$. The reconstruction process by FCPSE is relatively straightforward compared with the iterative CS-based coefficient estimation process by greedy algorithms or optimization algorithms, thus can realize lower computational costs.

Algorithm 3 Fast compressed power spectrum estimation [31]

Input: $\mathbf{Y}$; C;
Output: $\hat{\boldsymbol{\theta}}$

1: $h[n]\begin{cases}Y(i,j), n=jN+c_i\\ 0, \quad\quad \text{otherwise}\end{cases}$, $I[n]\begin{cases}1, n=jN+c_i\\ 0, \quad \text{otherwise}\end{cases}$
2: $\overline{h}[n]\begin{cases}h[n], & 0\le n\le LN-1\\ 0, & -LN+1\le N<0\end{cases}$,
$\overline{I}[n]\begin{cases}I[n], & 0\le n\le LN-1\\ 0, & -LN+1\le N<0\end{cases}$
3: $\boldsymbol{r}_h=\mathbb{F}^{-1}(|\mathbb{F}(\overline{\boldsymbol{h}})|^2)$, $\boldsymbol{q}=\mathbb{F}^{-1}(|\mathbb{F}(\overline{\boldsymbol{I}})|^2)$
4: $r_x[k]=r_h[k]/q[k]$, $k=-LN+1,-LN+2,\cdots,LN-1$
5: $\hat{\boldsymbol{\theta}}=\mathbb{F}(\boldsymbol{r}_x)$

4 Test Setup

GBSense Challenge 2021, as well as GBSense project itself, are distinguished by the combination of algorithm and hardware platform. In this section, we introduce a self-developed experimental platform for testing algorithms and generating test datasets. The test datasets utilized to evaluate the algorithms are then introduced briefly.

4.1 Data Collection Platform

The test datasets for GBSense Challenge 2021 were generated by a self-developed sub-Nyquist data processing platform. The platform was developed on the hardware basis of NI millimeter-wave transceiver system and LabVIEW software environment [9]. A general overview of the platform is shown in Figure 2. The platform is composed of a pair of chassis serving as the transmitter and the receiver. The transmitter has a baseband of [-1,1]GHz. Up to 8 transmissions with a maximum of 100MHz bandwidth can be generated simultaneously upon customized central frequencies over the baseband. The baseband signal is upconverted to 28.5GHz millimeter-wave band and emitted via a horn antenna. On the receiver side, the signal is first downconverted to baseband then demodulated in quadrature mode. A dual-channel high-speed ADC of 3.072GSPS sampling rate is utilized to digitize the signal in both in-phase and quadrature channels. The snapshots of the sample stream are captured and processed by the host CPU.

At software level, the sampling sequences is first interpolated to 2GSPS by Whittaker–Shannon method, then a multicoset sampler is simulated by discarding Nyquist samples according to the delay patterns. The simulated muticoset parameters (L, P and C)can be configured arbitrarily. Two greedy algorithms, SOMP and JB-HTP, are implemented for spectrum reconstruction, and the reconstruction results are plotted on the monitor in real time. At meantime, a reserved developer interface is provided for fast evaluation of other CSS algorithms.

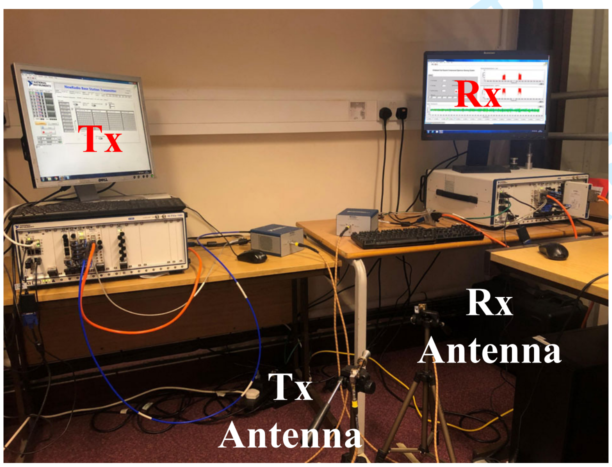

Fig. 2 Sub-Nyquist data collection and processing platform developed on the basis of NI millimeter-wave transceiver system.

4.2 Test datasets

Depending on the user's preference, the data storage function can operate prior to or after the multicoset sampler. For the GBSense Challenge 2021, Nyquist sample sequences at the input of the multicoset sampler are directly collected and released, allowing for greater parameter setting flexibility. For reference, both MATLAB and LabVIEW demo programs for multicoset sampling and SOMP/JP-HTP algorithms are made available alongside the datasets. Following is a brief description of the test datasets used during testing.

Test set 1 Test dataset published with the announcement of GBSense Challenge 2021 (24 pieces of data in total).

Test set 2 Gaussian-distributed spectrum, with SNR of 10dB and sparsity of 7.5% ~ 20% (100 pieces of data in total).

Test set 3 Gaussian-distributed spectrum, with SNR of 5dB and sparsity of 7.5% ~ 20% (100 pieces of data in total).

Test set 4 Gaussian-distributed spectrum, with SNR of 2dB and sparsity of 7.5% ~ 20% (100 pieces of data in total).

Test set 5 OFDM signal, with SNR of 10dB and sparsity of 7.5% ~ 15%. The original data is pseudo-random integer arrays, and the modulation method is QPSK (100 pieces of data in total).

Test set 6 OFDM signal, with SNR of 5dB and sparsity of 7.5% ~ 15%. The original data is pseudo-random integer arrays, and the modulation method is QPSK (100 pieces of data in total).

Test set 7 OFDM signal, with SNR of 2dB and sparsity of 7.5% ~ 15%. The original data is pseudo-random integer arrays, and the modulation method is QPSK (100 pieces of data in total) .

5 Numerical Results

The algorithms shortlisted for the GBSense Challenge 2021 have undergone various numerical tests for a thorough evaluation based on the competition's criteria. In this section, typical detection performance and time complexity data are shown.

Using a simulated 16-channel multicoset sampler($p = 16$), each piece of data in the aforementioned datasets is sampled. Each channel's sampling rate is 1/40 of the Nyquist rate ($L = 40$). The codes of the shortlisted entries are embedded to reconstruct the spectrum and of each piece of data. To avoid the reconstruction errors imposed by the delay pattern ,which are not the subject of this evaluation work, a large number of randomly generated delay patterns are utilized in the simulation, and their correspondintg results are averaged. Specifically, the test result on each piece of data is averaged using 100 random sampling delay patterns (except for FCPSE, which has a uniquely developed delay pattern creation module).

For each dataset, the reconstruction accuracies of the shortlisted algorithms are measured by the average Area Under Curve (AUC) of the receiver operating characteristic curve (ROC).

To reveal comprehensive features of the shortlisted algorithms, additional simulations are conducted. Typical ROC curves for the shortlisted algorithms under the aforementioned settings and 10dB SNR are shown in Figure 3. For the $k = 6$ case in Figure 3(a), the SBL and SK methods generally outperform the other greedy algorithms and non-sparse FCPSE algorithm. That is because the strong time correlation of the signal is utilized by SBL, and the global minimum is better approached by optimization problems. For the $k = 8$ case in Figure 3(b), a significant performance drop occurs for the SK algorithm. Note that $k = 8$ is the theoretical upper

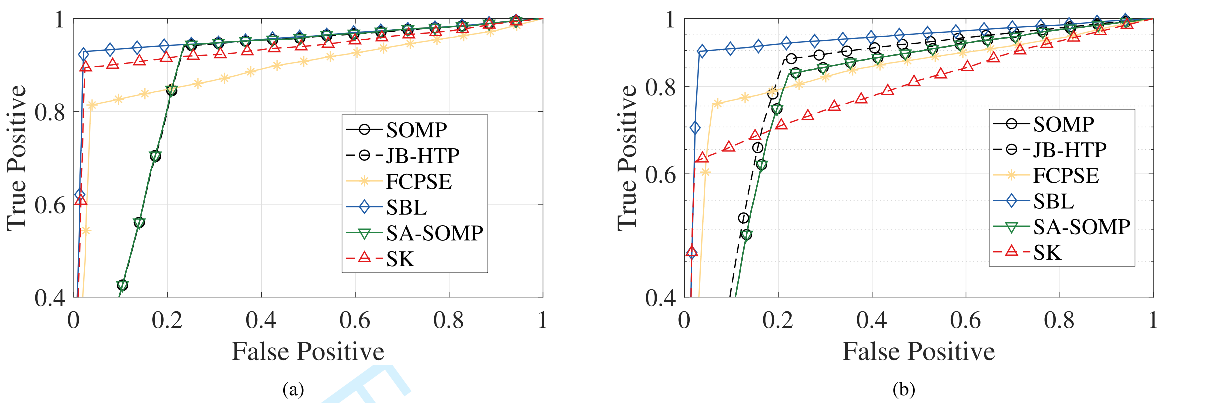

Fig. 3 Typical ROCs for the GBSense shortlisted algorithms compared with traditional SOMP and JB-HTP ($L = 40$, $p = 16$) on signal with sparsity (a) $k = 6$ and (b) $k = 8$.

bound for ensuring a unique solution with $p = 16$, which means this direct l_0-minimization strategy is vulnerable to sparsity change. It is also worth noting that JB-HTP tends to have better detection performance than SOMP when k increases because the misselected atoms can be fixed as the iteration of JB-HTP goes on, while a mismatch in SOMP cannot be excluded in the following iterations and will lead to slow convergence. SA-SOMP achieves exactly the same results as SOMP does because they share the same reconstruction strategy, and their only difference is the choice of the measurement matrix.

The shortlisted algorithms are tested for their detection probabilities defined by

$$P_d = \frac{\text{total \# correctly detected channels}}{\text{\# total active channels in all recovery trials}}. \quad (13)$$

under multiple SNR levels with $L = 40$, $p = 16$ and signal sparsity of $k = 6$, and the results are shown in Figure 4. Note that because FCPSE provides a non-sparse recovery, an additional screening of the $\hat{k}$ channels with the highest energy are kept as the recovered support. Among the curves in Figure 4, SK is the most sensitive method to noise which only achieve detection probability over 0.9 when $SNR \geq 10dB$. On the contrary, FCPSE is more resilient to noise level changes because Gaussian noise can be effectively damped by its statistical nature. However, detection probability above 0.9 is difficult to be achieved by FCPSE because the unbiased estimation is not always a good approximation, especially with sub-Nyquist samples and narrow sampling windows. SBL algorithm can achieve nearly 0.95 detection probability when $SNR \geq 5dB$ and 100% when $SNR \geq 10dB$, which outperforms the other algorithms within the simulation data.

For signal with different sparsity k from 1 to 16, simulations are conducted with $L = 40$, $p = 16$ and $SNR = 20dB$, and the results are shown in Figure 5. Taking advantage of the strong time correlation of the testing data, SBL outperforms the other algorithms on detection probability. The SK

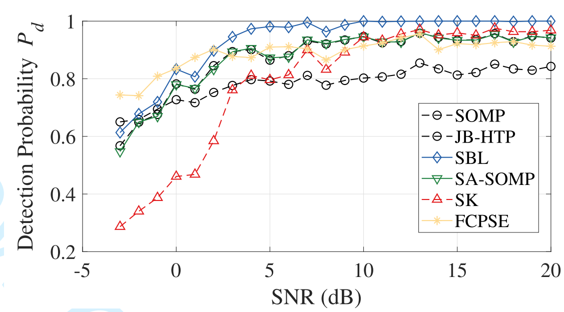

Fig. 4 Detection probability versus signal SNR for the four shortlisted algorithms compared with traditional SOMP and JB-HTP

algorithm performs well under $k \leq 6$ but quickly deteriorates when k gets larger. SOMP and SA-SOMP provide better results than JB-HTP when $k < 8$ but get worse when $k > 8$ because the atomwise matching is more accurate when fewer atoms are contributing to the signal but unreliable when a large number of weighted atoms are mixed. FCPSE gives a relatively detection probability for $k > 8$ than the greedy algorithms and SK.

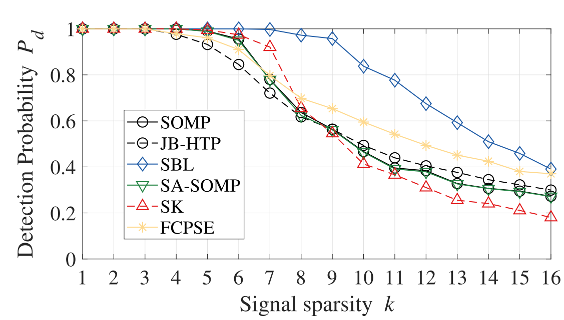

Fig. 5 Detection probability versus coset number p for the four shortlisted algorithms compared with traditional SOMP and JB-HTP

Table 1 Average AUC & running time on the GBSense test sets

Algorithm	AUC	Time (ms)
SBL	0.9771	3.5103
SA-SOMP	0.8190	1.3999
SK	0.6277	23.9034
FCPSE	0.8631	1.3734

As spectrum sensing is a task of high real-time requirement, the time complexity of a reconstruction algorithm is of great significance to be considered taking into practice. The time efficiency of the algorithms is measured by the average running time of the codes in MATLAB simulation. The test results for the four shortlisted algorithms are provided in Table 1.

By varying the length N of the sub-Nyquist sampling window, the real running time of each shortlisted algorithm on the CPU is tested by MATLAB, and the results are shown in Figure 6 in logarithmic coordinates, which in general agrees with Table 1. SK, as a l_0-optimization method, has naturally computational complexity orders higher than the other candidates. The SA-SOMP method achieves exactly the same detection results as SOMP but only costs running time comparable with JB-HTP, thus can be regarded as a promising method to be applied in very sparse conditions to achieve both high detection rates and high real-time performance. SBL costs moderate calculation time among the tested algorithms. The running time of three greedy algorithms and SBL is not sensitive to the increase of sampling window length N because they process the columns in the coefficient matrix $\mathbf{X}$ as joint-sparse. By contrast, the running time of FCPSE increases nearly exponentially with N because of the large amount of convolution included.

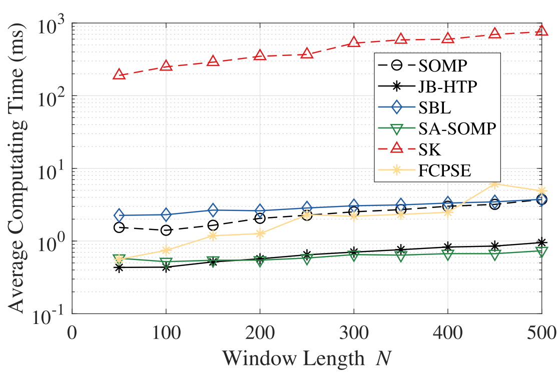

Fig. 6 Average running time versus the length N of the sampling window.

6 Conclusion

Utilizing the sparsity of the wideband spectrum, CSS offers a more effective method for reducing cognitive device reliance on energy-intensive, costly hardware. This study provides a brief introduction of the CSS framework based on multicoset sampling and introduces several widely used CS reconstruction techniques, including the greedy algorithm, optimization algorithm, sparse Bayesian learning algorithm, and non-sparse reconstruction algorithm. Four shortlisted algorithms for the GBSense Challenge 2021 are presented in detail and evaluated numerically.

Among the selected algorithms, SK gets a high detection rate under high SNR conditions, but has the lowest computational efficiency. SA-SOMP achieves satisfactory detection rates while maintaining a low computational complexity. FCPSE is capable of non-sparse spectrum reconstruction, but its precision is dependent on time frames that are longer. MSBL is capable of achieving precise spectral reconstruction under the Gaussian assumption and has acceptable computational efficiency. The numerical results are instructive for the practice of wideband compressed spectrum sensing.

From the perspective of real-world application, the future improvement of the spectrum reconstruction algorithm will primarily concentrate on the following: designing more stable reconstruction algorithms with lower computational complexity and lower average sampling rate requirements; designing effective reconstruction algorithms to accurately reconstruct the spectrum under Gaussian or non-Gaussian noise; designing targeted and feasible reconstruction algorithms.

7 Acknowledgement

Supported by the Engineering and Physical Sciences Research Council of United Kingdom under the Grant EP/R00711X/2.

References

1. Ahmad A, Ahmad S, Rehmani M H, Hassan N U, A survey on radio resource allocation in cognitive radio sensor networks, IEEE Communications Surveys & Tutorials, 17(2), 2015, 888–917
2. Mitola J, Cognitive radio : an integrated agent architecture for software defined radio, Thesis Kth Royal Inst Technology, 2000
3. Tropp J A, Laska J N, Duarte M F, Romberg J K, Baraniuk R G, Beyond Nyquist: Efficient sampling of sparse bandlimited signals, IEEE transactions on information theory, 56(1), 2009, 520–544
4. Yoo J, Becker S, Loh M, Monge M, Emami-Neyestanak A, A 100MHz–2GHz 12.5x sub-Nyquist rate receiver in 90nm CMOS, in: Proceedings of Radio Frequency Integrated Circuits Symposium, 2012
5. Eldar Y C, Sampling theory: Beyond bandlimited systems, Cambridge University Press, 2015
6. Mishali M, Eldar Y C, From theory to practice: Sub-Nyquist sampling of sparse wideband analog signals, IEEE Journal of Selected Topics in Signal Processing, 4(2), 2010, 375–391

7. Mishali M, Eldar Y C, Dounaevsky O, Shoshan E, Xampling: analog to digital at sub-Nyquist rates, Circuits Devices & Systems Iet, 5(1), 2009, 8–20
8. Venkataramani R, Bresler Y, Perfect reconstruction formulas and bounds on aliasing error in sub-Nyquist nonuniform sampling of multiband signals, IEEE Transactions on Information Theory, 46(6), 2000, 2173–2183
9. Song Z, Qi H, Gao Y, Real-time Multi-Gigahertz Sub-Nyquist Spectrum Sensing System for mmWave, in: Proceedings of the 3rd ACM Workshop on Millimeter-wave Networks and Sensing Systems, 2019, 33–38
10. Urkowitz H, Energy detection of unknown deterministic signals, Proceedings of the IEEE, 55(4), 1967, 523–531
11. Tandra R, Sahai A, SNR walls for signal detection, IEEE Journal of Selected Topics in Signal Processing, 2(1), 2008, 4–17
12. Oner M, Jondral F, Cyclostationarity-based methods for the extraction of the channel allocation information in a spectrum pooling system, in: Proceedings of 2004 IEEE Radio and Wireless Conference (IEEE Cat. No. 04TH8746), IEEE, 2004, 279–282
13. Cohen D, Eldar Y C, Sub-Nyquist cyclostationary detection for cognitive radio, IEEE Transactions on Signal Processing, 65(11), 2017, 3004–3019
14. Candes E J, Romberg J K, Tao T, Stable signal recovery from incomplete and inaccurate measurements, Communications on Pure and Applied Mathematics: A Journal Issued by the Courant Institute of Mathematical Sciences, 59(8), 2006, 1207–1223
15. Qi H, Zhang X, Gao Y, Low-Complexity Subspace-Aided Compressive Spectrum Sensing Over Wideband Whitespace, IEEE Transactions on Vehicular Technology, 68(12), 2019, 11762–11777
16. Eldar Y C, Kuppinger P, Bolcskei H, Block-sparse signals: Uncertainty relations and efficient recovery, IEEE Transactions on Signal Processing, 58(6), 2010, 3042–3054
17. Chen W, Wassell I J, A decentralized Bayesian algorithm for distributed compressive sensing in networked sensing systems, IEEE Transactions on Wireless Communications, 15(2), 2015, 1282–1292
18. Tropp J A, Gilbert A C, Signal recovery from random measurements via orthogonal matching pursuit, IEEE Transactions on information theory, 53(12), 2007, 4655–4666
19. Tropp J A, Gilbert A C, Strauss M J, Simultaneous sparse approximation via greedy pursuit, in: Proceedings.(ICASSP'05). IEEE International Conference on Acoustics, Speech, and Signal Processing, 2005., volume 5, IEEE, 2005, v–721
20. Needell D, Tropp J A, CoSaMP: Iterative signal recovery from incomplete and inaccurate samples, Applied and computational harmonic analysis, 26(3), 2009, 301–321
21. Palomar D P, Eldar Y C, Convex optimization in signal processing and communications, Cambridge university press, 2010
22. Mishali M, Eldar Y C, Blind multiband signal reconstruction: Compressed sensing for analog signals, IEEE Transactions on signal processing, 57(3), 2009, 993–1009
23. Liu R, Ma Y, Zhang X, Gao Y, Deep learning-based spectrum sensing in space-air-ground integrated networks, Journal of Communications and Information Networks, 6(1), 2021, 82–90
24. Zhang H, Yang J, Gao Y, Machine Learning Empowered Spectrum Sensing under a Sub-sampling Framework, IEEE transactions on wireless communications, 2022
25. Gao Y, Song Z, Zhang H, Fuller S, Lambert A, Ying Z, Mähönen P, Eldar Y, Cui S, Plumbley M D, et al., Sub-Nyquist spectrum sensing and learning challenge, Frontiers of Computer Science, 15(4), 2021, 1–5
26. She Y, Wang J, Li H, Wu D, Group iterative spectrum thresholding for super-resolution sparse spectral selection, IEEE Transactions on signal Processing, 61(24), 2013, 6371–6386
27. She Y, Wang Z, Shen J, Gaining Outlier Resistance With Progressive Quantiles: Fast Algorithms and Theoretical Studies, Journal of the American Statistical Association, 2021, 1–14
28. She Y, On the finite-sample analysis of \ *Theta*-estimators, Electronic Journal of Statistics, 10(2), 2016, 1874–1895
29. Ma Y, Zhang X, Gao Y, Joint sub-Nyquist spectrum sensing scheme with geolocation database over TV white space, IEEE Transactions on Vehicular Technology, 67(5), 2017, 3998–4007
30. Wipf D P, Rao B D, An empirical Bayesian strategy for solving the simultaneous sparse approximation problem, IEEE Transactions on Signal Processing, 55(7), 2007, 3704–3716
31. Yang L, Fang J, Duan H, Li H, Fast compressed power spectrum estimation: toward a practical solution for wideband spectrum sensing, IEEE Transactions on Wireless Communications, 19(1), 2019, 520–532
32. Tropp J A, Wright S J, Computational methods for sparse solution of linear inverse problems, Proceedings of the IEEE, 98(6), 2010, 948–958
33. Chen S S, Donoho D L, Saunders M A, Atomic decomposition by basis pursuit, SIAM review, 43(1), 2001, 129–159
34. Gorodnitsky I F, Rao B D, Sparse signal reconstruction from limited data using FOCUSS: A re-weighted minimum norm algorithm, IEEE Transactions on signal processing, 45(3), 1997, 600–616
35. Figueiredo M A, Nowak R D, Wright S J, Gradient projection for sparse reconstruction: Application to compressed sensing and other inverse problems, IEEE Journal of selected topics in signal processing, 1(4), 2007, 586–597
36. Wright S J, Nowak R D, Figueiredo M A, Sparse reconstruction by separable approximation, IEEE Transactions on signal processing, 57(7), 2009, 2479–2493
37. Zayyani H, Babaie-Zadeh M, Jutten C, Decoding real-field codes by an iterative Expectation-Maximization (EM) algorithm, in: 2008 IEEE International Conference on Acoustics, Speech and Signal Processing, IEEE, 2008, 3169–3172
38. Ji S, Xue Y, Carin L, Bayesian compressive sensing, IEEE Transactions on signal processing, 56(6), 2008, 2346–2356
39. Wipf D P, Rao B D, Sparse Bayesian learning for basis selection, IEEE Transactions on Signal processing, 52(8), 2004, 2153–2164

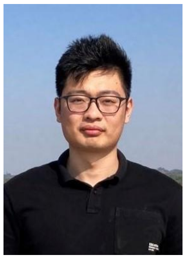

Zihang Song received his bachelor's and master's degrees in Applied Physics from Beihang University, China. He started his PhD study in 2019 and is now with Prof. Yue Gao and Prof. Rahim Tafazolli in University of Surrey, UK. His current research interests include millimeter-wave spectrum sensing and sub-Nyquist signal processing.

Han Zhang received his Ph.D. degree in Electrical and Electronics Engineering from University of California, Davis, Davis, California, USA, in 2019. He is currently working as a research assistant in the University of Surrey, Guildford, United Kingdom. His research interests include utilizing data driven methods on telecommunication scenarios, such as transceiver design and compressive sensing.

Sean Fuller is a Senior Account Manager at NI, specialised in wireless communications, data acquisition, and data analytics. He focuses on fostering collaborative relationships between industry and academia, with the goal of accelerating innovation. He received his Batchelor of Engineering (Hons) from the University of Portsmouth, UK.

Andrew Lambert (CEng FIET MIoD, Founder and CEO of Electronic Media Services Ltd and Founder and COO of Fibre Ltd) is a Chartered Engineer and Fellow of the Institution of Engineering Technology. He is an experienced board-level executive with a proven record of developing new technology to solve business problems with extensive practical experience of working in Europe and Asia.

Zhinong Ying is a principle researcher of Antenna technology in the Network Technology Lab within the Research Centre, Sony Cooperation, Lund, Sweden, also as a distinguish engineer within the whole Sony group. He joined Ericsson AB in 1995 in Sweden. He became Senior Specialist in 1997 and Expert in 2003 in his engineer career at Ericsson. He also has been a part time professor in department of electronic system, Aalborg University, Denmark since 2021. He is a Fellow of IEEE. He was a member of scientific board of ACE program (Antenna Centre of Excellent in European 6th frame) from 2004 to 2007.

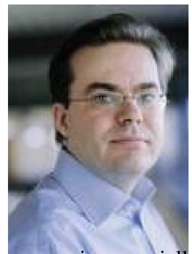

Petri Mähönen is currently a Full Professor and the Chair of Networked Systems with RWTH Aachen University. His current research interests include cognitive radio systems, embedded intelligence, and future wireless networks architectures, including millimeter-wave systems and techno-economics especially from a regulatory perspective. He is also serving as an Editor for the IEEE Transactions on Wireless Communications. He is also co-recipient of IEEE Jack Neubauer Memorial Award and received Telenor Research Prize for his work on spectrum related research.

Yonina C. Eldar is a Professor in the Department of Mathematics and Computer Science, Weizmann Institute of Science, Rehovot, Israel, where the heads the center for biomedical engineering. She was previously a Professor in the Department of Electrical Engineering at the Technion, where she held the Edwards Chair in Engineering. She is also a Visiting Professor at MIT, a Visiting Scientist at the Broad Institute, and an Adjunct Professor at Duke University and was a Visiting Professor at Stanford. She is a member of the Israel Academy of Sciences and Humanities, an IEEE Fellow and a EURASIP Fellow. She is the Chief Editor of Foundations and Trends in Signal Processing and a member of several IEEE Technical Committees and Award Committees.

Shuguang Cui received his Ph.D from Stanford in 2005. He is now a Chair Professor at The Chinese University of Hong Kong, Shenzhen. His current research interest is data driven large-scale information analysis and system design. He was selected as the Thomson Reuters Highly Cited Researcher and listed in the Worlds' Most Influential Scientific Minds by Sciencewatch in 2014. He was the recipient of the IEEE Signal Processing Society 2012 Best Paper Award. He is an IEEE Fellow and ComSoc Distinguished Lecturer.

Mark Plumbley is Professor of Signal Processing at the Centre for Vision, Speech and Signal Processing (CVSSP) and Head of School of Computer Science and Electronic Engineering at the University of Surrey, in Guildford, UK. He is an expert on analysis and processing of audio, using a wide range of signal processing and machine learning methods. He led the first international data challenge on Detection and Classification of Acoustic Scenes and Events (DCASE 2013), and is a co-editor of the recent book on "Computational Analysis of Sound Scenes and Events" (Springer, 2018). He currently holds a 5-year EPSRC Fellowship on "AI for Sound", aiming to bring sound recognition technology "out of the lab" for the benefit of society.

Clive G. Parini joined Queen Mary as Lecturer in 1977, promoted to Reader in 1990, promoted to Professor in 1999 and is currently Professor of Antenna Engineering and heads the Antenna & Electromagnetics Research Group. He has published over 400 papers on research topics including array mutual coupling, array beam forming, antenna metrology, microstrip antennas, millimetrewave compact antenna test ranges, millimetrewave integrated antennas, metamaterials and on-body communications. He is a Fellow of the IET and a past member and Chairman of the IET Antennas & Propagation Professional Network Executive Team. He is a past member of the editorial board and past Honorary Editor for the IET Journal Microwaves, Antennas & Propagation. In 2009 he was elected a Fellow of the Royal Academy of Engineering.

Arumugam Nallanathan is Professor of Wireless Communications and the founding head of the Communication Systems Research (CSR) group in the School of Electronic Engineering and Computer Science at Queen Mary University of London since September 2017. He was with the Department of Informatics at King's College London from December 2007 to August 2017, where he was Professor of Wireless Communications. He was an Assistant Professor in the Department of Electrical and Computer Engineering, National University of Singapore from August 2000 to December 2007. He has been selected as a Web of Science (ISI) Highly Cited Researcher in 2016. He is an IEEE Fellow and IEEE Distinguished Lecturer.

Yue Gao is a Professor and Chair in Wireless Communications at the Institute for Communication Systems, School of Computer Science and Electronic Engineering, University of Surrey, United Kingdom. He received a Ph.D. degree from the Queen Mary University of London. He leads the Antennas and Signal Processing Lab developing fundamental research into practice in the interdisciplinary area of smart antennas, signal processing, spectrum sharing, millimeter-wave and Internet of Things technologies in mobile and satellite systems. He has published over 200 peer-reviewed journal and conference papers, 1 book, and 5 book chapters. He is an Engineering and Physical Sciences Research Council Fellow from 2018 to 2023. He was a co-recipient of the EU Horizon Prize Award on Collaborative Spectrum Sharing in 2016.